

Easy Fabrication of Electrically Insulating Nanogaps by Transfer Printing

Omar Fakhr,* Philipp Altpeter, Khaled Karrai,* and Paolo Lugli*

An easy and cost-effective method to reproducibly fabricate nanogaps over a large area is introduced. Gold is evaporated on low-aspect-ratio polydimethylsiloxane (PDMS) stamps at an angle of 60°. Afterwards, the stamp is brought into contact with a silicon/silicon dioxide substrate and subsequently peeled at rates varying from 1 to 3 mm s⁻¹, resulting in the fabrication of nanogaps between two gold electrodes. The fabrication of insulating nanogaps with a width down to 50 nm is demonstrated.

1. Introduction

The experimental demonstration of single molecules providing electronic functionalities is gathering wide and increasing interest.^[1] A first exploitation of such a concept will probably arise from a hybrid system combining mainstream silicon technology with novel molecular devices.^[2] In order to satisfy the requirements for molecular scale integration in silicon technology, reliable fabrication techniques for nanometer-spaced electrodes are needed. Furthermore, the research on such systems requires the fabrication of electrodes with nanometer gaps. Several approaches in creating such gaps have been presented; however, these methods require extensive preparation processes and cannot achieve a uniform distribution over large areas.^[2]

Many lithography methods that allow fabrication of devices in the nanometer range require expensive instrumentation or processing costs, such as e-beam lithography, or immersion photolithography. The most cost-effective methods in creating downscaled devices over large areas involves the use of stamping techniques, such as nanoimprint lithography

(NIL)^[3] and soft lithography.^[4] The latter uses soft elastomeric stamps for nanofabrication. The use of soft lithography in creating unconventional micrometer- and nanometer-sized structures has risen exponentially since its initial use in 1993 by Kumar et al.^[5] Several methods and techniques can be performed using this technology, such as microcontact printing (μ CP),^[5] where self-assembled monolayers (SAMs) act as a resist for subsequent etching, and transfer printing,^[6] where thin films and objects are transferred additively onto a substrate. The most commonly used elastomeric stamp is made of soft polydimethylsiloxane (sPDMS), and cannot reach resolutions down to 250 nm.^[7] To overcome these limitations, several studies were conducted, which lead to new materials such as hPDMS (or hard PDMS)^[7] and regiflex molds.^[8] Other approaches for realizing structures in the sub-100-nm range involve using unconventional techniques, such as edge lithography,^[9] overpressure contact printing,^[10] or nanotransfer edge printing.^[11]

One attractive approach relying on elastomeric stamps is nanotransfer printing (nTP) of thin metal films.^[6] Here, a metal film, usually gold, is evaporated onto a structured stamp. This is brought into conformal contact with a functionalized surface of a target substrate, and then peeled off. Due to the difference in adhesion forces, where the substrate has more favorable surface energy than the stamp, the patterned thin metal film can be transferred. Thereby, ready-made structures of metal electrodes can be easily fabricated on top of a substrate, with no need of etching or lift-off processes. The transfer can be performed on various substrates, such as Si, SiO₂, plastic foils, or organic semiconductors.^[6,12,13] The use of SAMs to functionalize the surface of the substrate is often used to promote the transfer.

In this paper we present an nTP approach to create gaps in the sub-100-nm range using flexible stamps without the use of SAMs, ensuring thereby a gap without contamination of alien molecules, which can alter future measurements. The method we are presenting is very cost-effective and reproducible. It

O. Fakhr, K. Karrai
attocube systems AG
Königinstr. 11a RGB, 80539, Munich, Germany
E-mail: omar.fakhr@suss.com; Khaled.Karrai@attocube.com

O. Fakhr, Prof. P. Lugli
Lehrstuhl für Nanoelektronik
Technische Universität München
Arcisstrasse 21, 80333, Munich, Germany
E-mail: lugli@tum.de

P. Altpeter
Lehrstuhl für Festkörperphysik
Ludwig-Maximilians-Universität München
Geschwister-Scholl-Platz 1 80539 Munich, Germany

DOI: 10.1002/sml.201100413

ensures the creation of gaps over a large area, and provides the ability to fabricate different gap widths on a single substrate.

2. Results and Discussion

In its liquid viscous form, the PDMS stamp is mixed in a 10:1 ratio with its curing agent and cast against a hard template. Depending on the desired feature size, this template can be fabricated using expensive methods such as e-beam lithography, or by simpler photolithography. In our case, we fabricated the templates from 2-inch silicon wafers with conventional photolithography, having minimal relief size of 5 μm . After dry etching, the template structures had a height of 50 nm and an aspect ratio (height/width) of <0.01 . After replica molding with PDMS, we obtained low-aspect-ratio structures with very low elasticity, **Figure 1**. The recessed regions have a width w (varying from 5 to 50 μm) and a height of 50 nm. For metal deposition, we placed the PDMS stamp in a thermal

evaporator, under a pressure of 1×10^{-6} mbar. The plane surface of the stamp was placed at an angle of $\alpha = 60^\circ$ with respect to the line of sight of the tungsten boat. We evaporated a thin layer t of gold (40 nm) followed by a 4 nm thick layer of titanium. Titanium serves as an adhesion promotion layer to assist the transfer of the metal. The angle α guarantees that an area of the stamp of $l = t \cos\alpha$ is metal-free due to shadowing effect of the sidewalls.

PDMS stamps are very elastic and therefore susceptible to deformation. Consequently upon printing, the recessed regions of the low-aspect-ratio stamp also get into contact with the substrate. After peeling, the whole area is transferred, except for the shadowed areas, which contain no metal. This results in a metal-free nanogap, confined between two gold electrodes (metal pads). As the other sidewall facing the evaporation flux is covered with a thicker metal layer metal, protruded gold lines are formed upon transfer, as can be seen in the illustration in Figure 1D.

In initial attempts, PDMS stamps were peeled by hand from the substrate, and no gap was established as seen in **Figure 2a**. A thin metal layer takes the place of the desired

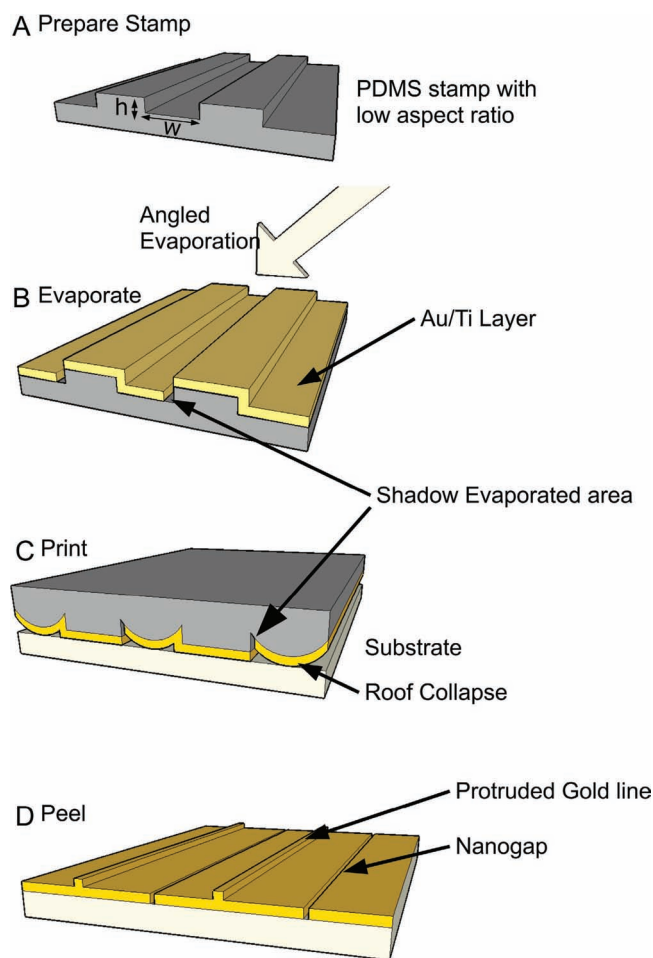


Figure 1. A PDMS stamp with low aspect ratio is evaporated with gold and titanium at an angle of 60° . The sidewalls facing the evaporation flux obtain a higher amount of gold, whereas the ones opposing it are poorly evaporated. When the evaporated stamp gets into contact with a substrate (Si or SiO_2) roof collapse allows the recessed regions of the stamp to get also into contact; after peeling gold is transferred onto the substrate, whereas parts of the sidewalls, that were badly covered, result in a nanogap, while the other sidewalls result into a protruded line with a typical height of 20 nm.

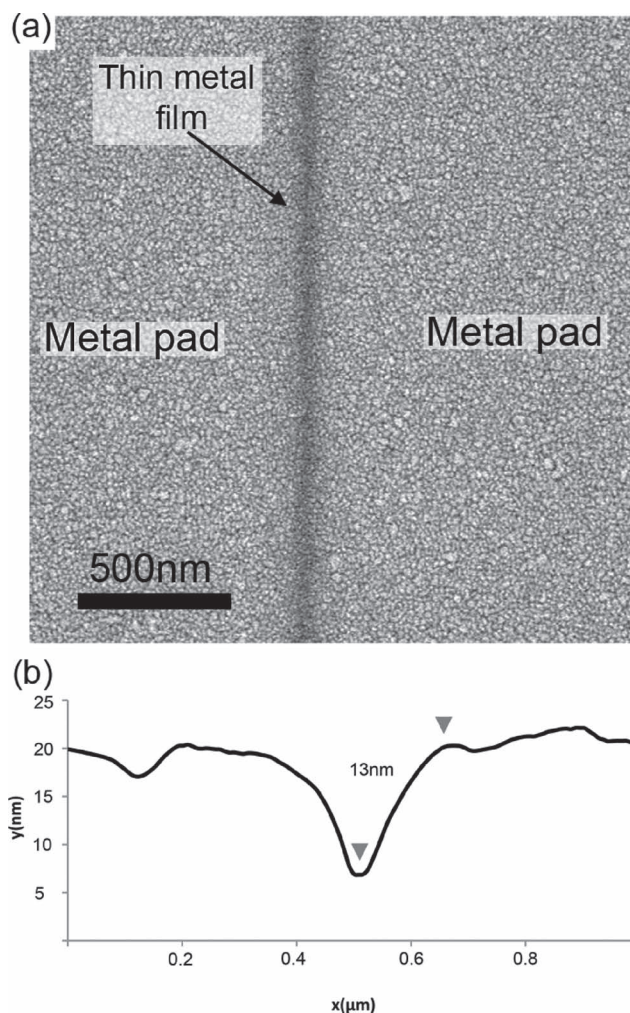


Figure 2. a) Scanning electron microscopy (SEM) image of a transferred metal film; the stamp was peeled by hand, the area of the gap contains a thin metal film. b) Atomic force microscopy (AFM) profile line of the thin metal film shows a decreased thickness of about 13 nm.

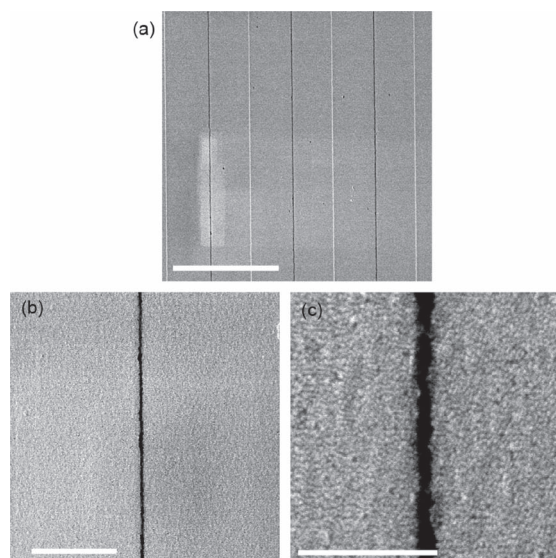


Figure 3. SEM images of printed gold on SiO_2 . The original template had $10\ \mu\text{m}$ lines at a $20\ \mu\text{m}$ period with a $50\ \text{nm}$ height. Evaporation was performed at an angle of 60° and a Au/Ti evaporated thickness of $40\ \text{nm}/4\ \text{nm}$; The sample was tilted 30° in the SEM with respect to the plane. a) A large view of the transferred structures, showing the resulting gaps and protrusions periodically. Scale bar: $20\ \mu\text{m}$. b) Magnified view of the gap, showing an insulating gap width between 50 and $80\ \text{nm}$. Scale bar: $2\ \mu\text{m}$. c) Magnified view of the gap with an average width of $57\ \text{nm}$. The morphology of the gold indicates agglomerates, which could not be seen with AFM measurements. Scale bar: $500\ \text{nm}$.

nanogap. The thickness in this area is smaller than the surrounding pads, as seen in Figure 2b.

As a peeling speed of $1\ \text{mm/s}$ using our self-designed printing machine, well-defined nanogaps were fabricated. **Figure 3** shows SEM images of the resulting nanogaps, fabricated by nTP. The master template had $10\ \mu\text{m}$ lines with $10\ \mu\text{m}$ separation, which means the gaps and lines are located at alternately with a $10\ \mu\text{m}$ distance. The width of the gaps is approximately $50\ \text{nm}$; whereas for the utilized geometry (60° evaporation angle and $50\ \text{nm}$ relief height), the nominal shadow area on the stamp should be around $86\ \text{nm}$. The protruded lines have a width of about $70\ \text{nm}$ and a height of $25\ \text{nm}$.

The reason for the discrepancy lies within i) the “roundness” of the PDMS and ii) the peeling mechanism. For any PDMS stamp, even with high aspect ratios, the edges of the structures are rounded.^[14] This is due to surface tension of the PDMS stamp. When the stamp is peeled from the master, the edges of the PDMS reach a smooth equilibrium. This edge radius was calculated to be $50\ \text{nm}$ for PDMS, which decreases with increasing elasticity modulus.^[14] **Figure 4a** shows an AFM image of the sidewalls of both the template and stamp. In order to avoid discrepancies between the two AFM measurements, we used the same tip geometry, same scanning speed, and same feedback loop parameters. The sidewall of the PDMS is flatter than the template; the structure height is decreased, and the edges are smoother. **Figure 4b** shows a schematic description of our process: gold is evaporated at an angle of 60° with respect to the plane. The sidewalls facing the evaporation flux receive higher amount of gold. The opposing sidewalls are nevertheless

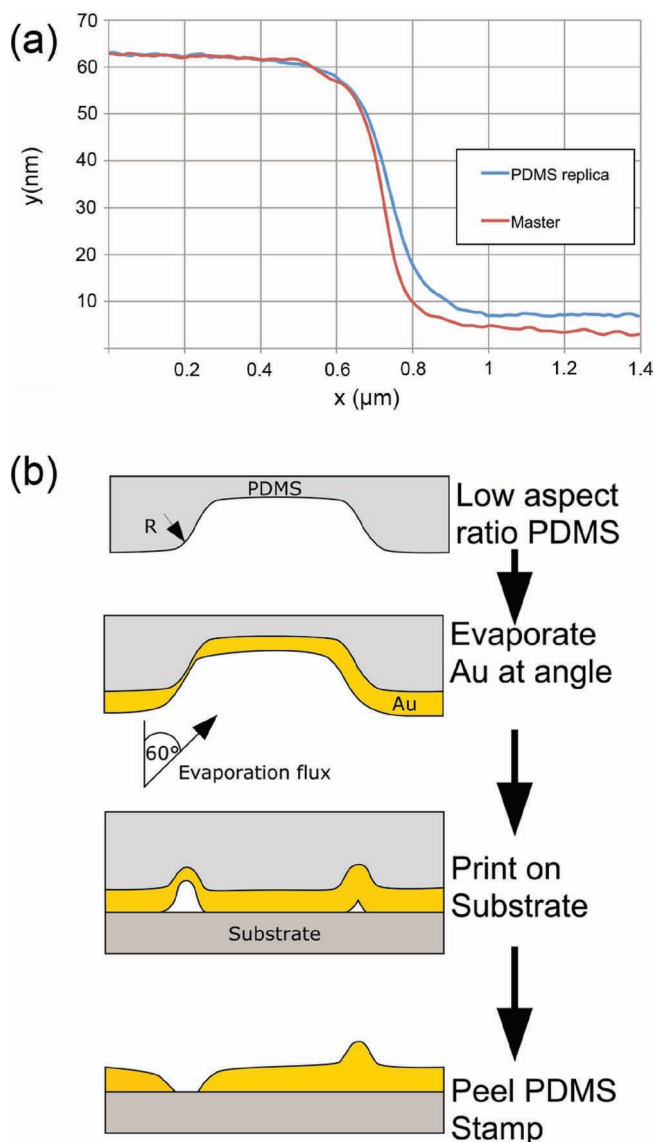


Figure 4. a) AFM images of both the sidewalls of the master template and the PDMS replica. The sidewalls of the replica are smoother and flatter than the template, suggesting PDMS reaches equilibrium due to surface tension. b) Detailed representation of the process: due to the flat sidewalls, the one opposing the evaporation flux is covered with gold. When printed, roof collapse occurs in the middle and spreads due to adhesion forces. When the stamp is correctly peeled, the poorly covered sidewall is ripped from the substrate, resulting in a nanogap.

not completely shadowed, as the ideal case of vertical sidewalls. When the stamp gets in contact with the substrate, the roof of the recessed regions collapses due to adhesion forces. The initial contact between the recessed region and the substrate occurs in the middle part and spreads laterally to the edges. The edges do not get into contact with the substrate.^[10] Nevertheless by conventional and slow hand peeling, the flat sidewalls can get into contact with the substrate, leading to the transfer of the thin metal film located at the sidewalls, and no gaps are created, as seen in Figure 2. The thickness of the metal in that area is lower than the surrounding parts, but not electrically insulating. In order to get metal-free gaps, the thin metal layer at the sidewall needs

to be “ripped” off the substrate by the peeling mechanism. It has been proven that adhesion of objects and thin films unto viscoelastic stamps depends on the peeling speed;^[15,16] i.e., peeling at low speeds leads to transfer of thin films and small objects onto the substrate (printing), whereas fast peeling can move objects from the substrate onto the stamp (pick-up). In order to fracture the thin film on the sidewall, thereby avoiding its adhesion to the substrate, the peeling energy has to exceed this of the cohesive energy of the thin metal film. It is to be noted that the thickness at the sidewall is gradual; i.e., varying the peeling speed leads to a variable fracturing point. Therefore, the width of the final gap can be controlled by the metal thickness and its gradient on the sidewall as well as the kinetic energy employed during peeling. Reproducible and defect-free gaps were fabricated using our automated self-made soft lithography aligner, which will be presented in a different publication. The device allows adjustment of the peeling speed from <0.3 to >3 mm/s. By peeling our PDMS stamps (evaporated with 40 nm gold and 4 nm titanium at an angle of 60°) at approximately 1 mm/s, we were able to obtain a nanogap width of 55 nm. Increasing the speed led to increasing the gap width up to 120 nm (peeling speed of approximately 2 mm/s) using the same stamp dimensions and the same evaporation angle. Higher peeling speeds do not allow transfer of the metal film.

We furthermore attempted achieving gaps with widths less than 50 nm by i) fabricating templates with smaller relief height of 25 nm and ii) by decreasing the evaporation angle to 45° . In both cases we were not able to get metal-free gaps. In the first case, the PDMS replica has very flat sidewalls due to its surface tension. Compared to higher reliefs, these sidewalls face a higher amount of gold (4 nm lower than the surrounding parts). This relatively thick film was difficult to fracture and did not produce nanogaps. The same is the case with stamps evaporated at 45° . In this method, nanogaps are obtained by shadow evaporation, where one sidewall receives less metal than the opposing one. This means that at any given evaporation angle, there is always a counterpart that connects the metal electrodes. **Figure 5a** shows an SEM image of the end of the gap structures. It can be observed that gold covers the whole area around the gap, thereby connecting the metal pads. To overcome this limitation, we performed another photolithography process on top of the low-aspect-ratio template. We structured lines on SU-8 passivation polymer with a thickness of 1.6 μm , perpendicular to the lines of the template, as depicted in **Figure 5b**. By replicating this template with PDMS, we were able to cut off the low-aspect-ratio structures with higher lines. During printing, these lines did not come into contact with the substrate, thereby the electrodes between the gaps are separated and do not form a short circuit. The separated lines had a typical depth of >4 μm , which can be easily fabricated using SU-8 polymer.

Figure 6a,b shows a set of gaps, 30 or 4 μm deep with a 5 μm separation. This technique allows for the fabrication of thousands of nanogaps on a single substrate, which are electrically isolated from each other. As seen in **Figure 6c–e**, we were able to fabricate nanogaps from approximately 55 to 120 nm by varying the peeling speed from 1 to 3 mm/s. Lower

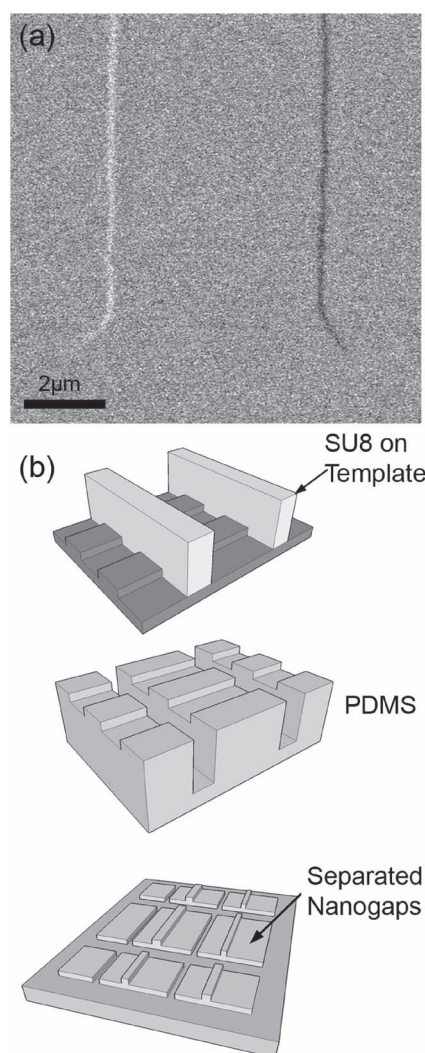


Figure 5. a) SEM image of the end of the gap: the electrodes surrounding the gaps are connected at the end, making a short circuit. b) An illustration of creating trenches between the gaps to avoid short circuits: by performing photolithography on top of the low-aspect-ratio structures of the template, higher structures can be fabricated. By replicating this template, trenches are obtained in the PDMS stamp and do not get into contact to the substrate.

peeling speeds can lead to bridges that can short circuit the gap, as seen in **Figure 6f**. Typical widths of such a metal bridges are about 8–10 nm, thereby having very low conductivity. The exact correlation between the peeling speed and the width of the gap is currently under investigation.

Figure 7 shows a comparison of the current–voltage (I – V) characteristics between two 50 μm wide, 22 nm thick transferred thin metal films, one of which has a 50 nm gap. Both films were transferred by the same process on silicon dioxide. For this measurement, we used conventional probe tips for contacting the thin metal film. The tips caused considerable scratching of the metal film, resulting in increased contact resistance and decreased current density. Nevertheless, the electrical measurement of the gap shows only noise. As a result we proved that our metal transfer method is conductive and that the nanogaps are insulating.

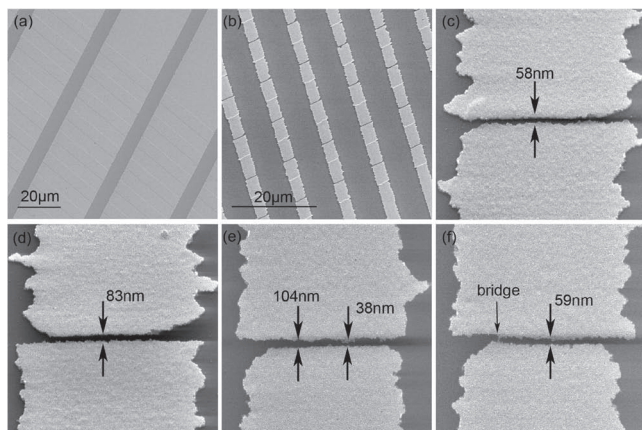


Figure 6. SEM images of a) nanogaps, 30 μm deep, separated by 5 μm trenches; b) nanogaps, 4 μm deep, separated by 10 μm trenches. c–e) Magnified images of nanogaps, with an average width of 58 (c), 83 (d), and 104 (e) nm. The sample in (e) has a part reaching down to 38 nm, but still perfectly insulating. f) Magnified image of a nanogap with a bridge connecting the two electrodes. This bridge is approximately 10 nm wide.

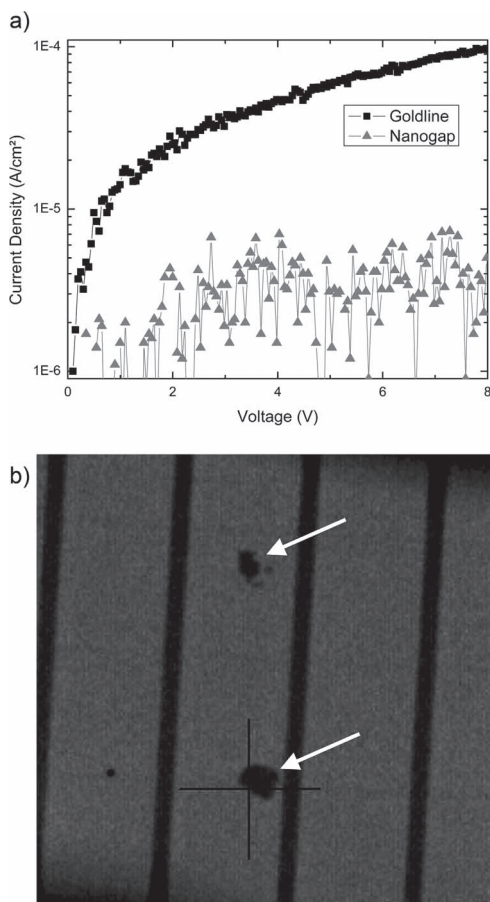


Figure 7. a) Conductivity measurement of a transferred thin film with 50 μm line width and a 22 nm thick metal layer. The measurement of the gap was conducted at the same geometry, i.e., same distance of probe pins (100 μm). The value of the idle current of the connected line is the same as the gap. b) Optical microscope image showing the placement of the probe tips at a distance of approximately 100 μm (highlighted by the arrows). The pins cause scratches in the metal film and result in high contact resistance.

3. Conclusion

In this study we presented a method of creating nanogaps on silicon and quartz surfaces. This method is very cost-effective, reproducible, and very easy to fabricate. It also has the advantage of obtaining thousands of electrically separated nanogaps with different widths on the same substrate. The nanogaps can be varied from 55 to 120 nm by varying the peeling speed. Smaller nanogap widths could demand templates with re-entrant walls, in order to obtain near vertical sidewalls and thereby have greater control over the shadow-evaporated area.

4. Experimental Section

Fabrication of Templates: Templates were fabricated using photolithography on silicon wafers, followed by reactive ion etching using SF₆ (Oxford Plasmalab 80) at 25 mTorr for 24 s.

Fabrication of PDMS Stamps: PDMS (Sylgard 184 from Dow Corning) was mixed in a 10:1 ratio with its curing agent and degassed in an exicator for 1 h. Afterwards it was spin-coated on the template at 2000 rpm for 10 s. The poly-foil as a backing layer was previously placed in a Diener plasma Asher for 30 s at 0.4 bar and 35 W power, to activate its surface. It was then placed gently on the spin-coated PDMS to avoid air bubbles. All was placed on a hot plate at 65 °C for 4 h to cure the PDMS. Afterwards the stamp was peeled from the template and placed on the stamp holder, designed for our soft lithography aligner.

Evaporation: PDMS stamps were placed at a 60° angle from the line of sight of the tungsten boats containing the metals in an evaporation machine and 1×10^{-6} mbar vacuum was applied. Gold (40 nm) was evaporated followed by 4 nm of titanium at rates of 0.1 and 0.04 nm/s, respectively.

Printing and Peeling: After evaporation the stamp holder containing the stamp was placed in our aligner and brought in contact with the substrate. After 3 min, the PDMS stamp was peeled at rates varying between 1 and 3 mm/s.

Characterization: For our SEM images we used an LEO SEM. For AFM, we used a Joel AFM with standard tips purchased from Nanosensors with a tip radius of <10 nm. Electrical characterization was performed using probe tips (Cascade) and a Keithley 2600 sourcemeter.

Acknowledgements

The authors would like to thank Bernhard Fabel, Mario Bareiß, and Andreas Hochmeister for their help in the IV-measurements, Thomas Zabel, and Linda Mora for their help for fabricating the template, and Werner Krauß for technical advice. Partial financial support of the Institute of Advanced Study of the Technische Universität München and of the DFG Excellence Cluster “Nanosystem Initiative Munich” is gratefully acknowledged.

- [1] A. Aviram, M. A. Ratner, *Chem. Phys. Lett.* **1974**, *29*, 277–283.
- [2] T. Li, W. Hu, D. Zhu, *Adv. Mater.* **2010**, *22*, 286–300.
- [3] S. Y. Chou, P. R. Krauss, P. J. Renstrom, *Appl. Phys. Lett.* **1995**, *67*, 3114.
- [4] Y. Xia, G. M. Whitesides, *Angew. Chem. Int. Ed.* **1998**, *37*, 550–575.

- [5] A. Kumar, G. M. Whitesides, *Appl. Phys. Lett.* **1993**, *63*, 2002–2004.
- [6] Y. Loo, R. L. Willett, K. W. Baldwin, J. A. Rogers, *J. Am. Chem. Soc.* **2002**, *124*, 7654–7655.
- [7] H. Schmid, B. Michel, *Macromolecules* **2000**, *33*, 3042–3049.
- [8] D. Suh, S. Choi, H. H. Lee, *Adv. Mater.* **2005**, *17*, 1554–1560.
- [9] T. Cao, Q. Xu, A. Winkelman, G. Whitesides, *Small* **2005**, *1*, 1191–1195.
- [10] Guo Teng, H. Yang, *Nano Letters* **2004**, *4*, 1657–1662.
- [11] M. Xue, Y. Yang, T. Cao, *Adv. Mater.* **2008**, *20*, 596–600.
- [12] Y. Loo, J. W. P. Hsu, R. L. Willett, K. W. Baldwin, K. W. West, J. A. Rogers, *J. Vac. Sci. Technol. B* **2002**, *20*, 2853.
- [13] Y. Loo, R. L. Willett, K. W. Baldwin, J. A. Rogers, *Appl. Phys. Lett.* **2002**, *81*, 562.
- [14] C. Y. Hui, A. Jagota, Y. Y. Lin, E. J. Kramer, *Langmuir* **2002**, *18*, 1394–1407.
- [15] X. Feng, M. A. Meitl, A. M. Bowen, Y. Huang, R. G. Nuzzo, J. A. Rogers, *Langmuir* **2007**, *23*, 12555–12560.
- [16] M. A. Meitl, Z. Zhu, V. Kumar, K. J. Lee, X. Feng, Y. Y. Huang, I. Adesida, R. G. Nuzzo, J. A. Rogers, *Nat. Mater.* **2006**, *5*, 33–38.

Received: March 3, 2011

Revised: April 13, 2011

Published online: